ELSEVIER

Nuclear Instruments and Methods in Physics Research A 453 (2000) 17–24

NUCLEAR INSTRUMENTS & METHODS IN PHYSICS RESEARCH Section A

www.elsevier.nl/locate/nima

Hadron collider detectors

J. Incandela

Fermi National Accelerator Laboratory, Batavia IL, USA

Accepted 16 June 2000

Abstract

Experiments are being prepared at the Fermilab Tevatron and the CERN Large Hadron Collider that promise to deliver extraordinary insights into the nature of spontaneous symmetry breaking, and the role of supersymmetry in our universe. This article reviews the goals, challenges, and designs of these experiments. © 2000 Published by Elsevier Science B.V. All rights reserved.

PACS: 14.80.B; 14.80.C; 14.80.L; 29.40.Vj; 29.40.Wk; 29.40.Gx; 29.40.Cs; 29.40.Mc; 29.50. + v

Keywords: ATLAS; CDF; CMS; D0; Higgs; Supersymmetry

1. Introduction

The first hadron collider, the ISR at CERN, had to overcome two initial obstacles. The first was low luminosity, which steadily improved over time. The second was the broad angular spread of interesting events. In this regard Maurice Jacob noted [1]: "The answer is ... sophisticated detectors covering at least the whole central region ($45^\circ \leq \theta \leq 135^\circ$) and full azimuth." This statement, while obvious today, reflects the major revelation of the ISR period that hadrons have partonic substructure. The result was an unexpectedly strong hadronic yield at large transverse momentum (p_T). Partly because of this, the ISR missed the discovery of the J/Ψ and later missed the Υ. The ISR era was therefore somewhat less auspicious than it might have been. It did however make important contributions in areas such as jet production and charm excitation and it paved the way for the SPS collider, also at CERN.

The partonic substructure of colliding hadrons leads to multiple production mechanisms, ($q\bar{q}$, qq', qg, gg...) and a broad range of center of mass (CM) energies. This means that one can probe realms far above (or below) the average constituent CM energy, and study a very large array of topics. However, broadband production comes at a price. There is no beam energy constraint and the cross-sections for interesting processes are many orders of magnitude below the total inelastic cross-section (σ_{tot}). At Fermilab this is 60 mb and it will be 100 mb at the LHC, where a 500 GeV Higgs would have a production cross-section of $10^{-11}\sigma_{tot}$. High luminosities also mean multiple interactions per beam crossing. The LHC expects an average of 25 interactions per crossing at a luminosity of $10^{34}\,cm^{-2}\,s^{-1}$. This corresponds to the production of as many as 10^4 tracks every 100 ns [2].

Nevertheless, hadron collider experiments have been extremely successful, not only in the realm of

0168-9002/00/$ - see front matter
PII: S0168-9002(00)00601-X

new discoveries, but in precision measurements as well. The cross-section for production of the W at the SPS was $10^{-8}\sigma_{tot}$ at the time of its discovery [3,4]. Hadron collider experiments have since measured the W mass [5] to high precision: $M_W(\mathrm{CDF}\oplus\mathrm{D0}\oplus\mathrm{UA2}) = 80.448 \pm 0.062\,\mathrm{GeV}$. Similarly, $t\bar{t}$ production was discovered [6–8] at $10^{-10}\sigma_{tot}$ by CDF and D0 who then measured its mass [9] to high precision as well: $M_{top}(\mathrm{CDF}\oplus\mathrm{D0}) = 174.3 \pm 5.1\,\mathrm{GeV}$. The discovery of $t\bar{t}$ production is an example of how hadron colliders have exceeded expectations. The Tevatron delivered more data than expected, and good calorimetry and lepton identification enabled top events to be efficiently detected and well-reconstructed. In the case of CDF, a silicon vertex detector made it possible to select extremely pure event samples as shown in Fig. 1.

All hadron collider experiments currently in preparation have similar goals. Namely, the discovery of the Higgs boson and supersymmetric (SUSY) partners, precision masses and electroweak parameter measurements, and b physics. The latter includes measurements of the CKM matrix parameters, CP violation, and B_s mixing. To achieve these goals, sophisticated new detectors are required.

2. Collider experiments at the Fermilab Tevatron

Upgrades to the FNAL accelerator complex, including the addition of the new Main Injector, will ultimately increase luminosity by more than an order of magnitude and raise the CM energy 10% to 2 TeV. Previously, the luminosity peaked at $\sim 3\times10^{31}\,\mathrm{cm^{-2}\,s^{-1}}$ with bunch spacing of $\sim 3.5\,\mu\mathrm{s}$. In a first operating phase (Run 2a), the luminosity will reach $1\text{–}2\times10^{32}\,\mathrm{cm^{-2}\,s^{-1}}$ with a bunch spacing of 396 ns. In a later phase (Run 2b), the bunch spacing will be reduced to 132 ns and the luminosity will reach $5\times10^{32}\,\mathrm{cm^{-2}\,s^{-1}}$. It is expected that this scenario will enable each experiment to accumulate $15 \pm 5\,\mathrm{fb^{-1}}$ of data prior to the operation of the LHC. In order to match the higher collision rates of the accelerator, the detectors require new front end and trigger electronics.

The Tevatron experiments have some hope of discovering the Higgs boson because it is expected to be light. Fits to precision electroweak measurements [10] yield a central value near 100 GeV and an upper bound of order 250 GeV for the SM Higgs mass. The current lower limit from LEP is $\sim$ 100 GeV and will eventually reach 110 GeV. In addition, SUSY models predict a mass below 135 GeV for the lightest Higgs boson [11].

Direct production via gluon fusion is the dominant SM Higgs production mode [11]. At Fermilab these events will be overwhelmed by dijet backgrounds except perhaps for the case $H \to W^+W^- \to l^+l^-\nu\bar{\nu}$. Therefore, the associated production modes $qq' \to HW$ and $q\bar{q} \to HZ$ will be used. These have rates an order of magnitude lower, but also have much rarer backgrounds ($t\bar{t}$, $Wb\bar{b}$, $Zb\bar{b}$, WZ...). The dominant decay modes of the SM Higgs at low mass are $H \to b\bar{b}$ and $H \to W^+W^-$. Below about 130 GeV the former dominates and leads to $W(l\nu,qq') + b\bar{b}$ and $Z(l^+l^-,\nu\bar{\nu},q\bar{q}) + b\bar{b}$ final states. The $H \to W^+W^-$ mode dominates above 140 GeV and leads to

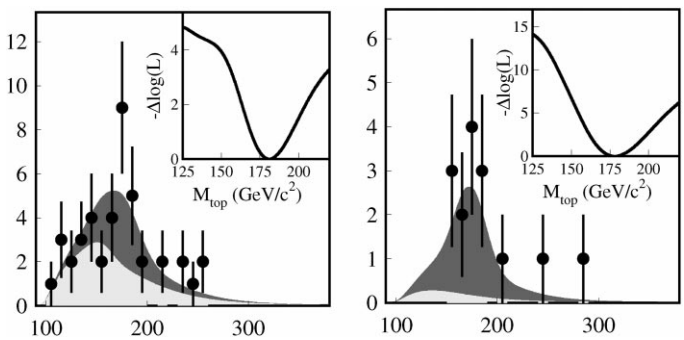

Fig. 1. Background (lightly shaded regions) in CDF top candidates before (left), and after requiring one b tag (right).

$W^+W^-, W^+W^-W^\pm, W^+W^-Z$ events with low backgrounds for the leptonic final states, (e.g. $l^+l^-\nu\bar{\nu}$, $l^+l^-\nu\bar{\nu}jj$, $l^+l^-l^+\nu\bar{\nu}\nu$ ...). Near $M_H = 135\,\text{GeV}$ the W^+W^- and $b\bar{b}$ decay modes are comparable and sensitivity is diminished.

The key experimental capabilities for these events are lepton identification, b tagging, and jet and missing energy resolution. This is also true for W, top, and bottom studies and many SUSY searches. Lepton coverage will be crucial to gluino pair production with cascade to like-sign di-leptons, or gauginos to tri-leptons. Lifetime tagging of bottom and charm could enable the detection of stop pair production with top-like decays or cascades to charm. To optimize their capabilities for b tagging, lepton identification, and energy resolution, both experiments have embarked upon extensive instrumentation upgrades.

2.1. The CDF upgrade

The CDF upgrade [12] includes silicon, a wire drift chamber (COT), a time-of-flight (TOF) detector, new endplug calorimeters, extended muon systems, and new front-end electronics, trigger, and DAQ. The goals of the 722k channel silicon system are to double b tagging coverage to $|\eta| \leq 2$, enable 3D vertexing and deadtime-less triggering on displaced tracks, and to improve impact parameter resolution. The core of the system is the SVX II detector which has five double-sided layers extending to $\pm 45\,\text{cm}$ from the center of the detector as necessitated by the broad span of interactions along the beam axis. SVX II will be used in a level 2 online trigger [13] enabling CDF to collect large samples of hadronic b decays as well as to tag long-lived particles in high p_T events. This allows reduced track momentum, jet energy, and missing energy thresholds for higher efficiency. Inside the SVX II and mounted directly on the beam pipe at a radius of 1.5 cm will be the Layer 00 silicon. This layer uses single-sided 25 μm pitch detectors with 50 μm readout pitch. The readout electronics will be outside the tracking volume. The silicon will be cooled to 5°C and can operate at high bias voltages as necessitated by radiation damage [14,15]. Layer 00 reduces uncertainty in the transverse impact parameter of tracks to $\sim 6 \oplus 20/p_T\,\mu\text{m}$. This leads to significant improvements in high p_T b tagging [15] in Higgs and top events, and in b physics. Just outside the SVX II is the ISL which is comprised of two layers of double-sided silicon (1.2° stereo) at radii of 20 and 28 cm. The ISL extends $\pm 95\,\text{cm}$ along the beam axis and enables tracking and b tagging to be extended to $|\eta| \leq 2$. In the central region, $|\eta| \leq 1$, the ISL is surrounded by the COT which is a wire drift chamber with 96 wire planes grouped into eight superlayers of which alternate layers are $\pm 3°$ stereo. Groups of 12 sense and 17 potential wires are contained in cells separated by Au-plated mylar sheets. Front-end electronics can measure charge deposition for particle identification. Further particle identification will be made possible by a TOF system [15] which is installed just beyond the COT. It is made up of scintillator bars read out at both ends by fine-mesh photomultipliers. The expected resolution is of order 100 ps and will enable kaon identification for b flavor tagging. For improved electron and jet finding in the forward region, as well as improved missing energy resolution, CDF has installed new scintillator-tile endplug calorimeters. These will have resolution comparable to the central calorimeters, namely $\sigma_E/E \sim 15/\sqrt{E}\oplus 7\%$ electromagnetic and $\sigma_E/E \sim 70/\sqrt{E}\oplus 4\%$ hadronic [12]. Outside the calorimeters, muon systems will be upgraded to fill holes and extend coverage.

The CDF Level 1 trigger has a pipeline of 42 cells allowing a 50 kHz accept rate. At Level 2, there is a 2 stage asynchronous pipeline comprised of 4 buffer cells to allow an accept rate of 500 Hz. At Level 3 a Linux processor farm will fully reconstruct events and select less than 50 per second for storage.

2.2. The D0 upgrade

The major D0 upgrades [16] include a 793k channel silicon microstrip vertexer, a central fiber tracker (CFT), a 2 T solenoid with a radius of 60 cm, enhanced muon systems, and all new front-end electronics, trigger, and DAQ. The D0 silicon includes '*F* disks' which reside between and just beyond the barrels, and '*H* disks' which are installed in the far forward regions. The barrels consist of

axial and either 90° or 2° stereo layers while the disks are either $\pm 15°$ (F) or $\pm 7.5°$ (H) symmetric u–v doublets. Surrounding the silicon is the 2.6 m long CFT [17] made up of eight layers of axial and $\pm 2°$ stereo doublets of 1 mm diameter scintillating fibers. The 77k fibers will be read with visible light photon counters (VLPC) operated at 8°C with $\leq 0.1\%$ noise occupancy. The axial layers will be used in a level 1 track trigger. The silicon and fibers are surrounded by a 2 T superconducting solenoid. The tracker will have good momentum resolution and impact parameter resolutions $\sigma_d(r\phi) \sim 12 \oplus 35/p_T$ and $\sigma_d(rz) \sim 40\,\mu m$. As for CDF in past runs, the tracking system will enable in situ calibration of the electromagnetic calorimeter using isolated electrons by comparing energy and momentum measurements. D0 will retain its existing hermetic LAr calorimeter which has resolution of $\sigma_E/E \sim 15\%/\sqrt{E}$ for electrons, $\sigma_E/E \sim 50\%/\sqrt{E}$ for pions, and $e/\pi \leq 05$ above 30 GeV. The total jet energy correction is 15% above 30 GeV – 200 GeV then falls to $\sim$12% at 400 GeV. There will also be improved forward and central preshower detectors. The central preshower will use 7 mm prismatic scintillator strips to reduce the electron trigger rate by a factor of 5. The calorimeters use switched capacitor arrays for pipelining data. The silicon and fiber readout use the SVX2 chip which has a 32 cell pipeline.The trigger/DAQ system will focus on regions of interest within events to avoid full event reconstruction. Level 0 is a beam crossing trigger (minimum bias). Level 1 is based upon calorimetry, preshower, CFT, and muon scintillators as well as some information on displaced tracks from the silicon system. It has a 5–10 kHz accept rate. Level 2 hardware trigger will have 1 kHz accept rate. Level 3 is a processor farm with 20–50 Hz accept rate. The event size will be $\sim$250 kB.

2.3. Expectations for Run 2

Studies indicate that the two experiments can combine results to make some significant statements about the Higgs [18,19]. For example, with 10 fb^{-1} per experiment the Higgs can be excluded to $M_H < 180$ GeV (95%CL). With 20 fb^{-1} per experiment a 3σ observation is possible up to 180 GeV and a 4σ discovery would be possible below 125 GeV or in the range 150–170 GeV. These results are summarized in Fig. 2. In the realm of SUSY, inroads will be made in a fair portion of the parameter space [20]. With 10 fb^{-1} per experiment, CDF and D0 will be able to combine to reach an uncertainty of $\sim$20 MeV in the W mass and $\sim$1 GeV uncertainty in the top mass. This will severely constrain the SM Higgs mass as seen in Fig. 2. For b physics, CDF expects to measure $\sin 2\beta$ to an uncertainty of 0.07 (0.02) for 2 (15) fb^{-1}. With the new TOF and Layer 00 systems, CDF will have unrivaled sensitivity to B_s mixing [15].

3. Collider experiments at the CERN LHC

The LHC will collide protons at 14 TeV CM energy. Initially, the luminosity will be $10^{33}\,cm^{-2}\,s^{-1}$ and later increase to $10^{34}\,cm^{-2}\,s^{-1}$. The bunch

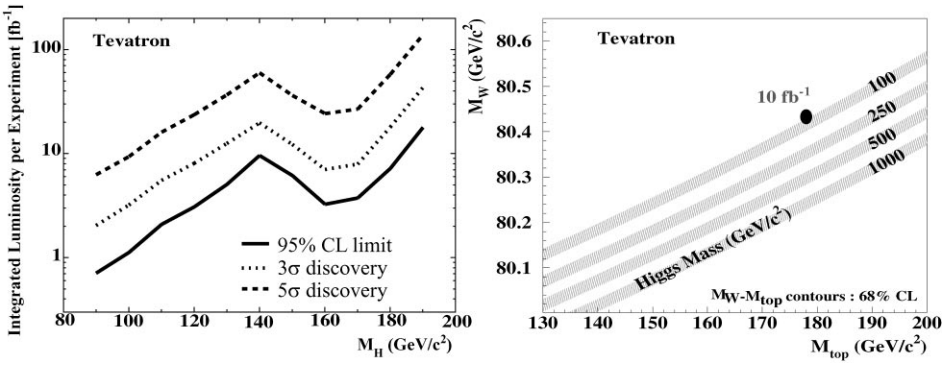

Fig. 2. CDF ⊕ DO sensitivity of Higgs via direct searches (left), and potential for constraining the SM Higgs mass (right).

spacing will be 25 ns. As for the Tevatron, SM Higgs production is dominated by gluon fusion. The cross-section for associated production with vector bosons, however, will be many orders of magnitude lower. In both cases the backgrounds will be larger than at the Tevatron. As a result, the LHC experiments are designed to have extremely good energy resolution for electrons and photons, as well as good momentum resolution for muons. This allows the Higgs to be observed as a narrow mass resonance on top of sometimes very large backgrounds. The specific modes considered relate to different mass ranges and to SM versus SUSY Higgs. At low mass, a SM Higgs will be sought via $H \to \gamma\gamma, b\bar{b}, ZZ^*$ where the latter leads to very clean four lepton final states. At intermediate and high masses (200 GeV – 1 TeV), the modes of interest are $H \to ZZ, WW$ with leptonic final states. For SUSY Higgs, all the modes just mentioned are useful but will be augmented by searches using, for example, τ final states [2]. Of course, the experimental capabilities relevant to Higgs searches also enable fairly comprehensive searches for SUSY partners, precision measurements of SM parameters, and searches for evidence of dynamical symmetry breaking and quark compositeness.

3.1. CMS

The CMS experiment [21] is anything but compact in overall size, as seen in Fig. 3. The CMS inner detector [22] includes two barrel pixel layers at radii of 4 and 7 cm for low luminosity and at radii of 7 and 11 cm for high luminosity running. There will also be two planes of forward pixels arrayed in disks. The individual pixels in all cases are 150 μm squares. Outside the pixels will be a silicon microstrip system made up of 10 barrel layers beginning at a radius of 21 cm. Layers 1,2,5,6 and 7 will be double-sided with 100 mrad stereo angle. In the forward regions there will be 10 disk planes per end, of which planes 1 and 10 will be double-sided stereo. All double-sided detectors are made up of single-sided detectors mounted back-to-back.

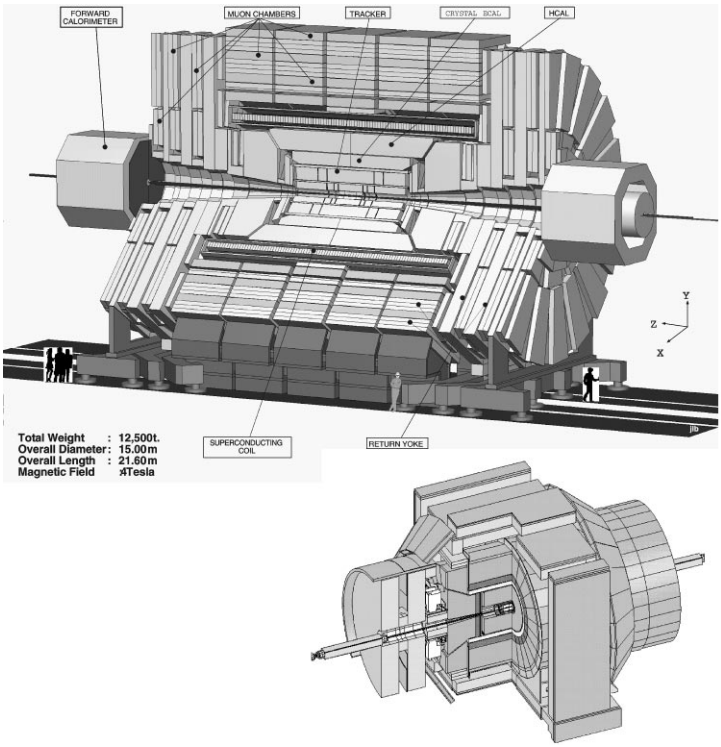

Fig. 3. The CMS detector with the CDF detector inset (to scale) for comparison.

The pixel and silicon systems extend to a radius of 1.3 m and to $\pm$ 3 m along the beam axis from the nominal center of the detector. The silicon has a surface area in excess of 240 m^2. The momentum resolution is expected to be $\sigma/p_T(\text{TeV}) \sim (15 \times p_T \oplus 0.5)$ % in the central region. For muons this improves to $\sim 4.5 \times \sqrt{p(\text{TeV})}$ %. The asymptotic transverse (longitudinal) impact parameter resolution will be better than 35 (75)μm for $|\eta| \leq 2.5$. The CMS calorimeters [21] include a $PbWO_4$ crystal electromagnetic calorimeter with Si avalanche photodiode readout surrounded by a Cu and scintillator-tile hadronic calorimeter. The calorimeters and tracking elements are inside a 4T solenoidal magnetic field. The electromagnetic calorimeter will have resolution of $\sigma(E)/E(\text{GeV}) \sim (2.7/E \oplus 0.55)$ % in the central region and $\sim(5.7/E \oplus 0.55)$ % forward. For a 130 GeV Higgs and 100 fb^{-1} of data, the decay $H \to \gamma\gamma$ can yield an uncertainty of less than 1 GeV on the mass.[1] Excellent resolution is also expected for $H \to ZZ \to e^+e^-e^+e^-$ events. Outside the calorimeters, the muon system, which extends from 3.9 m to 6.9 m radially, gives the detector its overall physical size. The golden channel $H \to ZZ \to \mu^+\mu^-\mu^+\mu^-$ will be extremely clean and yield a very precise mass. The CMS trigger will have input rates reduced to acceptance rates as follows; 40 MHz $\to$ 100 kHz at Level 1, $\to$ 10 kHz at Level 2, $\to$ 100 Hz at Level 3 for output to tape. As for the Tevatron experiments, the trigger will require extensive pipelining within the front-end electronics, and a large number of event builders. The event size is expected to be $\sim$1 MB resulting in $\sim$1 TB of data acquired daily.

3.2. ATLAS

ATLAS is the largest collider experiment ever to be undertaken [23,24]. Its physical size is also determined by its muon system which uses 20 m diameter air-core toroids and which has endcap planes separated by 46 m. The ATLAS inner detector starts with pixel layers with 50 μm × 300 μm pixels. In the central region there is one replaceable layer at roughly 4 cm radius and 2 additional fixed layers at larger radii. There will be five endcap disks per side. Outside the pixels there are four double-sided, shallow stereo barrel layers of silicon microstrips and nine endcap wheels per end. The total area of silicon is $\sim 61\,m^2$. Beyond the silicon will be a 36 layer, transition-radiation, straw-tube tracker with single hit resolution of 170 μm. The system will have impact parameter resolution $\sigma_d(r\phi) = 11 \oplus 60/p_T \sin\theta\,\mu\text{m}$ and $\sigma_d(rz) = 70 \oplus 100/p_T \sin^3\theta\,\mu\text{m}$. The ATLAS tracker will be contained within a 2T solenoid. The calorimeter includes a Pb-LAr accordion electromagnetic system in the central region surrounded by a scintillator-tile hadronic section. In the forward regions the electromagnetic and hadronic systems both use LAr. Preshower detectors are installed ahead of the electromagnetic calorimeter inside the solenoid cryostat wall and employ narrow strips to allow pointing to the interaction vertex with $50\,\text{mrad}/\sqrt{E}$ resolution. Overall the resolutions expected are $\sigma(E)/E = 10/\sqrt{E} \oplus 0.3\%$ in the central electromagnetic and $38/\sqrt{E} \oplus 1.6 \oplus 3.0/E$ % in the tile hadronic system. The muon system will provide momentum resolution of order 2–3% for intermediate momenta and $\sim$10% at 1 TeV. As for CMS, ATLAS energy and momentum measurements will enable excellent mass resolution. The ATLAS trigger/DAQ system, like that of D0, will focus on regions of interest within events to avoid full event reconstruction.

3.3. Expectations for LHC physics

With 100 fb^{-1} of data, both ATLAS and CMS expect to be able to discover a SM Higgs regardless of mass, as seen in Fig. 4. Both experiments will also have the capability to measure the Higgs mass to better than 1% accuracy and the width to better than 10% in most cases, although below a mass of $\sim$200 GeV the true width is smaller than the experimental resolution. It is expected that SUSY Higgs (e.g. the five Higgs bosons of the minimal SUSY extension of the SM) will be accessible to masses in excess of 500 GeV. ATLAS and CMS will be sensitive to SUSY partners with masses as high as 2 TeV in some cases and with 300 fb^{-1} could

[1] This assumes identification of the correct primary interaction vertex.

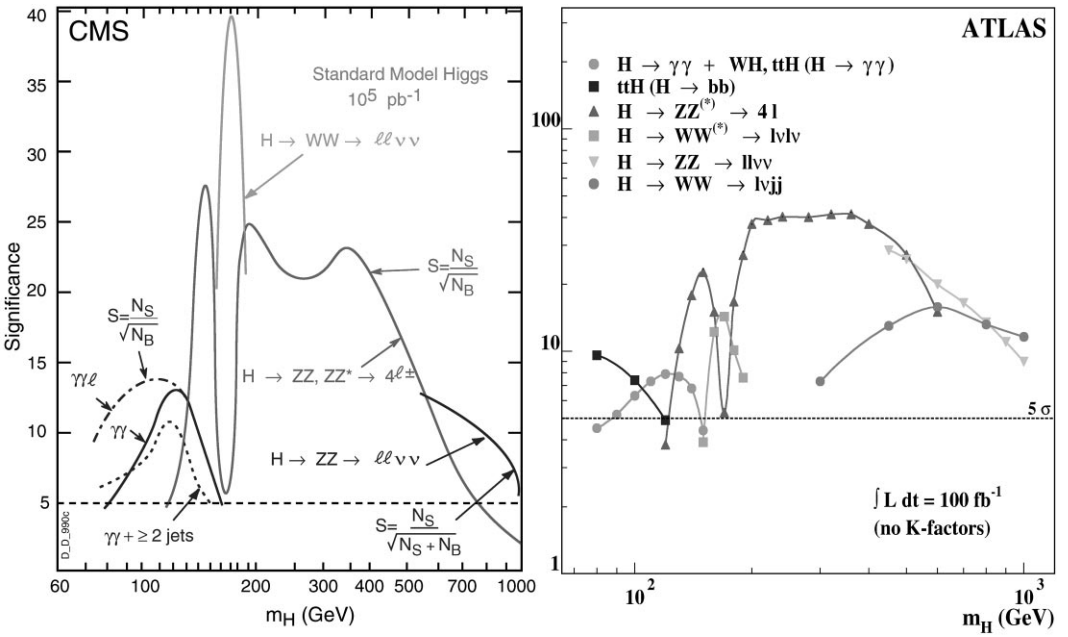

Fig. 4. The CMS and ATLAS expectations for SM Higgs discovery as a function of mass in 100 fb^{-1} of data.

detect quark compositeness at scales as high as 40 TeV.

4. Conclusions

Hadron colliders have come a long way since the days of the ISR and have now been established not only as premier discovery centers, but also as sources of precision measurements. Current multi-purpose experiments are in the midst of major construction projects which promise to yield detectors of unprecedented scale, complexity, and capability. These detectors will soon provide us with a deeper understanding of spontaneous symmetry breaking and the origin of mass. They will also determine the status of supersymmetry in our universe, and provide us with a large array of precision measurements of SM and beyond-SM parameters. These experiments have an unprecedented potential for discovery, making this the most exciting period in the history of hadron colliders.

I would like to thank V. Buescher, M. Dela Negra, D. Denegri, J. Goldstein, D. Green, K. Hara, C. Hill, P. Jenni, F. Lehner, G. Martin, H. Montgomery, T. Nelson, M. Roco, S. Stapnes, D. Stuart, and T. Virdee for providing useful information and comments, and also thank H. Incandela for help in preparing this document.

References

[1] M. Jacob, K. Johnsen, CERN 84-13, 1983.
[2] S. Tapprogge, ATL-CONF-99-004, 1999.
[3] G. Arnison et al., UA1 Collab., Phys. Rev. Lett. B 122 (1983) 103.
[4] M. Banner et al., UA2 Collab., Phys. Rev. Lett. B 122 (1983) 476.
[5] W. Carithers, FERMILAB-CONF-99-292-E, 1999.
[6] F. Abe et al., CDF Collab., Phys. Rev. Lett. 73 (1994) 225.
[7] F. Abe et al., CDF Collab., Phys. Rev. Lett. 74 (1995) 2626.
[8] S. Abachi et al., D0 Collab., Phys. Rev. Lett. 74 (1995) 2632.
[9] L. Demortier et al., CDF and D0 Collab., FERMILAB-TM-2084, 1999.
[10] LEP Electroweak Working Group http://www.cern.ch/LEPEWWG/.
[11] M. Spira, Fortschr. Phys. 46 (1998) 203.
[12] CDF II, Technical Design Report, FERMILAB-PUB-96/390-E, 1996.

[13] A. Bardi et al., Nucl. Instr. and Meth. A 409 (1998) 658.
[14] P. Azzi-Bacchetta et. al, CDF4924, 1999.
[15] Proposal for enhancement of the CDFII Detector, CDF5096, 1999.
[16] M. Roco, FERMILAB-CONF-98-268-E, 1998.
[17] M.R. Wayne, Nucl. Instr. and Meth. A 387 (1997) 278.
[18] J. Conway, FERMILAB-CONF-99-156-E, 1999.
[19] M. Roco, FERMILAB-CONF-99-240-E, 1999.
[20] H. Baer et al., Phys. Rev. D 54 (1996) 5866.
[21] Online documentation; http://cmsdoc.cern.ch/documents.html.
[22] CMS, The Tracker Project ..., CERN/LHCC-98-6, 1998.
[23] CERN-LHCC-99-14, 1999.
[24] I. Efthymiopoulos, Acta. Phys. Pol. B 30 (1999) 2309.